



A Study of Pressure Gradient during the Activity of 120-Day Winds of Sistan and its Relationship with Dust and Wind Speed in Helmand Basin, Iran

Fatemeh Dargahian^{1,*}, Mahdi Doostkamian²

¹ Desert Research Division, Research Institute of Forests and Rangelands (RIFR), Agricultural Research Education and Extension Organization (AREEO), Tehran, Iran

² Zanzan University, Zanzan, Iran

Received: 5 May 2021, Revised: 16 November 2021, Accepted: 26 December 2021

© University of Tehran

Abstract

120-day wind of Sistan is a regional wind current that blows on average from June to September. This wind, which is accompanied by dust, has carved its role on the face of the Sistan region due to its continuity and speed. This study aimed to investigate the pressure gradient during the activity of 120-day winds and its relationship with dust and wind speed in Helmand Endorheic basin. For this purpose, the dust and wind speed data of 11 synoptic stations were daily extracted from the Iran Meteorological Organization since 1986 for Helmand basin. After making a complete database, the frequency of dusty days and wind speed during the activity of 120-day winds of Sistan was extracted. Atmospheric pressure data corresponding to the duration of the activity of 120-day winds was extracted from the National Center of Environmental Prediction (NCEP) and National Center of Atmospheric Research (NCAR) databases with a spatial resolution of $2.5^\circ \times 2.5^\circ$. Following the extraction of pressure gradient via Pearson correlation coefficient, the relationship between the speed and dust of the basin, and the pressure gradient was investigated. The study of wind speed showed that strong winds during the activity of 120-day winds had an increasing trend. The results also revealed that the pressure gradient had a direct relationship with wind speed and dust storms in Helmand basin. In addition, the speed and dusts of the mid-eastern part of the basin were mostly influenced by the pressure gradient.

Keywords: Pressure gradient, Helmand, Correlation, Dust, Wind speed, Iran

Introduction

Dust storm is a meteorological phenomenon (Kaykhosravi and Haseli, 2017) and occurs in arid regions where strong winds separate dust particles from surface and scatter them (Arnes, 2012). Dust storm is a large cloud of dust sucked by a strong wind. Dust is primarily a combination of small-size particles that have ascended in to the atmosphere. Dust cloud is so dense that can block the sun and zero out the field of view in an area of hundreds or thousands of miles (Anaxos, 2008). Dust storm rises once the intensity of the wind passing through exceeds the threshold value. As a result, sand and removable dust is separated from the arid surface in these regions (Kaykhosravi and Haseli, 2017). The transportation of soil particles mostly depends on the wind speed while the size of particles has no relationship with the amount of transported dust; in other words, wind transports smaller particles in greater amount and larger particles in smaller amounts. Studies have shown that the required speed for particles transportation is about 20 km/h at a height of 30 cm (Refahi, 2009).

Iran is located in a belt where most of the world's arid and semi-arid regions happen to be (Alizadeh, 2009). Therefore, in case of winds blow at speeds above the threshold, dusts will be

* Corresponding author e-mail: dargahian@rifr-ac.ir

created and enter the atmosphere. Sistan is one of the windy regions in eastern Iran (Tavousi et al., 2012). Planetary speaking, this region is the borderline between tropical and subtropical atmospheric systems. Due to the interaction of pressure and temperature between these two circulation systems, strong winds blow in the region, known as 120-day winds (Saliqeh, 2010). These winds give rise to dust storms in the region. The pressure difference between the Afghanistan mountain range and Sistan plain is one of the causes of winds and dust storms in Sistan plain. From Iran's northeastern highlands to southeastern ones, these storms turn into a hot and dry wind in Sistan plain after passing through the deserts, causing serious damages to agricultural fields and vegetation. The blowing time of the winds giving rise to storms is usually from late May to late September (Tavousi et al., 2010). Over the recent decades, the occurrence of dust storms has increased due to climate changes as well as drought occurrence in different regions. In this regard, numerous studies have investigated dust storms and their relationship with climate changes; for example, Brazel and Nickling (1986) studied the association of weather and dust storms of Arizona. They reported that although dust storms can be traced to specific synoptic events, the internal variability of dust storms shows a strong correspondence to antecedent winter moisture variability, probably reflecting an overriding control by surface crusting and vegetative effects on dust generation. Miri et al. (2010) investigated the dust storms of Sistan after 1999 drought. Their result indicated a relationship between increasing drought occurrence and wind speed. Drought occurrence, increased wind speed, and Lake Hamoun dryness have severely intensified the dustiness in the region. Prakash et al. (2015) studied the impact of dust storms on the Arabian Peninsula and the Red Sea, whose result showed that the Arabian Peninsula, located in the dust belt, is a major source of atmospheric dust. Frequent dust outbreaks and approximately 15 to 20 dust storms per year have profound effects on all the aspects of human activity and natural processes in this region. Diaz and Sanchez (2016) analyzed the dust storm in Sahara. They found that mineral dust aerosols coming from the arid and semiarid regions of the world can aggregate and form microspherulites under special atmospheric conditions. Pokharel et al. (2017) studied extratropical storms of Sahara and reported that only the higher-resolution data sets can resolve the mesoscale processes, which are mainly responsible for creating strong low-level terrain-induced downslope winds, leading to the initial dust storms. There are a few previous works on the climatic control of dust storm frequency, especially in the field of time series analysis. In fact, there is poor correspondence of the mean values of climatic parameters and dust storm data. Although generally negative, rainfall and dust-storm correlations do not reveal the physical causes of dust storm generation, as shown by lagged cross-correlation and spectral analysis. Temperature data may indicate seasonal variation of dust storms by extreme values, but there are no reliable defining factors on account of the high persistence over shorter time series. The same has been found for the mean wind speeds while negative interrelations with atmospheric pressure highlight the importance of cyclogenesis and convective cells in dust storm generation in Asia (Littmann, 1991). Desert dust interacts with shortwave (SW) and longwave (LW) radiation, influencing the Earth radiation budget and the atmospheric vertical structure (Meloni et al., 2015). The emission and re-absorption of photoelectron and/or secondary electron at the walls of microcavities formed between neighboring dust particles below the surface are responsible for generating unexpectedly large negative charges and intense particle-particle repulsive forces to mobilize and lift off dust particles (Wang et al., 2016). The wind data showed that both are operating. The time domain shapes of the dust pulses are highly variable, but we have little understanding of what provides these shapes (Kellogg et al., 2016).

In Iran, Alijani and Raispour (2011) statistically and synoptically studied the dust storms of Sistan region and reported that cold air falling from the high pressure of the northern Caspian Sea to the region creates a dust storm. According to satellite image processing, the most important sources of dust are the dried substrates of Hamoon Puzak, Saberi and east of Hamoon

Helmand. Shahriari and Mohammadi (2015) investigated the trend of Sistan and Baluchistan dust phenomenon based on the nonparametric methods. Their primary results revealed that this method could be adapted for signifying the type of the existing trends. Additionally, all the stations had a positive trend in monthly and yearly periods. Meanwhile, in warm months (May, June, July, and August), positive trend were larger than that in other months. Raygani et al., (2016) identified the potential dust sources in Alborz province. The results showed that the combination of remote sensing and numerical simulation methods and field-based data could perfectly show active dust sources. Zeinali (2016) investigated the frequency of the changes in days with dust storms in the western half of Iran. They reported that the majority of the stations in the western half of Iran have an increasing trend of dust storms. It rose markedly in southwest of Iran. Jalali et al., (2017) identified dust storm sources and the affected areas by them in southwest of Iran. They showed that generally, satellite images and climatological and environmental data are used simultaneously in dust storm studies.

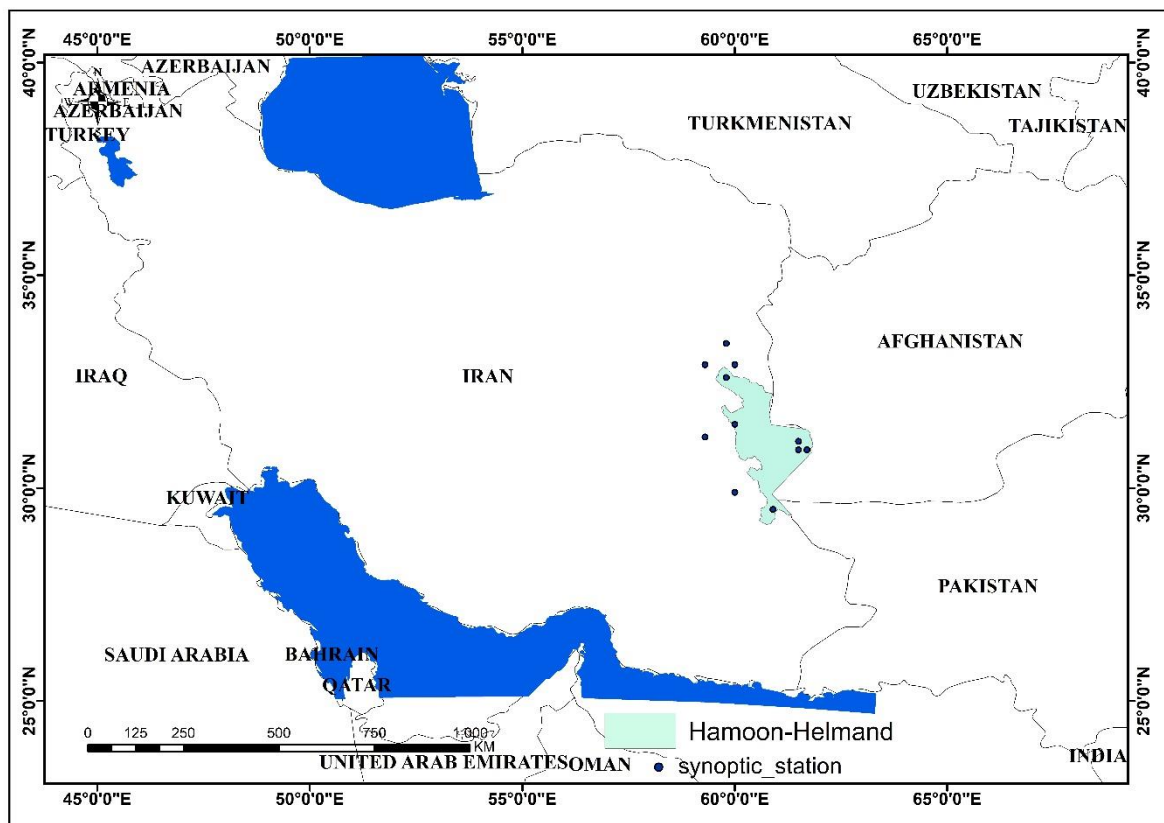
As it gets warmer in May, Iran's southeastern low-pressure domain extends and as a result, the embayment over the Caspian Sea draws eastward. At this time, the winds blowing from east and southeast, as 120-day winds, are the result of circulation and entrance of air towards the low-pressure part of southeastern Iran. It is the main sources of high-pressure winds over the Caspian Sea and the cold air of the Hindu Kush and the Himalayas. To put it in other words, as the high pressure over the Caspian Sea increases, it moves the air towards the low-pressure part in southeastern Iran. When high pressure withdraws or decreases over the Caspian Sea, the cold air of the Himalayas and Hindu Kush moves towards the low-pressure part of southeastern Iran. It initially has a northeastern direction, which, once reaching South Khorasan province, takes a northern direction. It finally deviates towards southeast of Sistan. Regarding wind performance, it is safe to say that on one hand, receiving solar energy is significant and on the other, the elevation-associated difference between low surfaces and marginal heights has led the plains to be always warmer than the adjacent mountains. As a result of this temperature difference, the pressure gradient of these surfaces is very high, causing the blow of almost constant daily or seasonal winds from the heights towards the plains. Apart from the local and regional winds, trans-regional winds, like 120-day winds, having almost a constant and definite season, direction, and intensity, contribute to the formation of desert in Iran (Zomordian, 2002). Most of the studies were exclusively conducted on statistical analysis of Sistan dust and wind speed. However, many researchers believe that the rising and occurrence of dust and winds storms are due to the pressure difference because of high pressure in northeastern Iran and the formation of low pressure in southern Iran and parts of Pakistan and Afghanistan. Therefore, the present study aimed to investigate the pressure gradient of these two systems and their effects on Helmand basin dusts. Thus, we sought to study the pressure gradient during the 120-day wind activity period and its relationship with dust and wind speed in the inner basin of Helmand watershed.

Materials and Methods

In this study, wind speed data and dust codes (06, 07, 08, 09, 30, 31, 32, 34, and 35) were extracted from Iran Meteorological Organization during 1986-2018 period for 11 synoptic stations in Helmand basin. The study aimed to investigate the pressure gradient during the activity of 120-day Sistan winds and its relationship with dust and wind speed in Helmand basin (Figure 1).

Table 1. Location of synoptic stations in and around the studied watershed

Station	Province	Latitude	Longitude	Elevation
Birjand	Southern Khorasan	32.9	59.3	1491
Nehbandan	Southern Khorasan	31.5	60	1188
Zabul	Sistan and Baluchestan	31.1	61.5	489.2
Zahedan	Sistan and Baluchestan	29.5	60.9	1370
Sarbisheh	Southern Khorasan	32.6	59.8	1846
Dehsalm	Southern Khorasan	31.2	59.3	815
Nusrat Abad	Sistan and Baluchestan	29.9	60	1127
Zahak	Sistan and Baluchestan	30.9	61.7	495
Hamoun	Sistan and Baluchestan	30.9	61.5	482.5
Darmeyan	Southern Khorasan	32.9	60	1553.8
Zahan	Southern Khorasan	33.4	59.8	1753.4

**Figure 1.** Geographical location of the study area

120-day winds start blowing from late May to late September in Sistan. Since we conducted the present research to investigate the relationship between the pressure gradient, dust, and wind speed during the activity of 120-day wind, only the wind and dust speed from 1986 to 2018 were considered. Iranian researchers believe that the occurrence of 120-days wind is due to Pakistan low-pressure extension (Gandmakar, 2009a; Gandmakar, 2010), pressure gradient between Pakistan low-pressure and Caspian high-pressure, topographic configuration and cold air transportation from the Himalayas and the Hindu Kush towards Sistan (Hosseinzadeh, 1997). In this regard, after preparing environmental data, ground surface pressure data corresponding to the wind and dusts speed data were extracted from NCEP and NCAR. The spatial resolution of these data was $2.5^\circ \times 2.5^\circ$. Figure 2 illustrates the pressure data for these points.

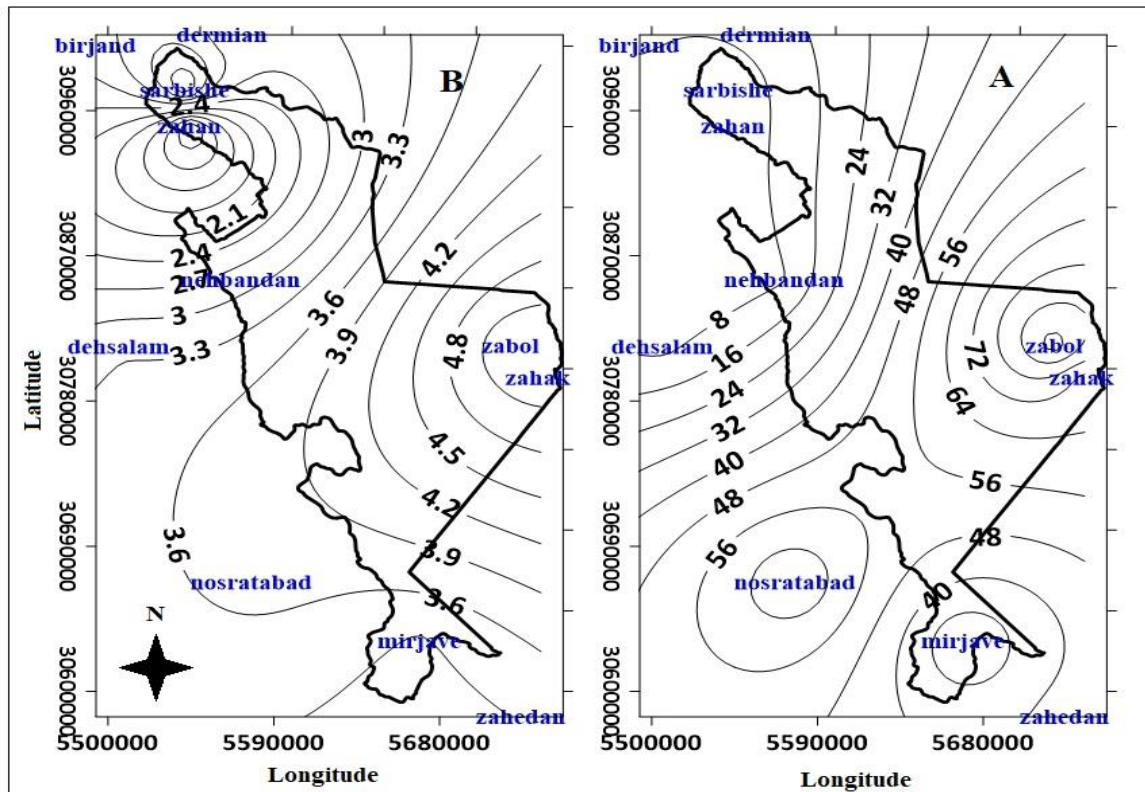


Figure 2. Spatial distribution of the studied stations and isobar lines, average dust (A) and wind speed (B)

Results and Discussion

Tables 1 and 2 represent some of the spatial characteristics of the high- and low-pressure centers during the activity of 120-day winds of Sistan. According to Table 1, the highest average pressure occurred in May 2007 with 1017.7 hPa. The highest and lowest coefficient of variation for the high-pressure centers was 3.3% in September and 4.4% in May, respectively (Table 1). Therefore, the beginning and end of the activity period of the Sistan 120-day winds had a high spatial coefficient of variation. In fact, the positive kurtosis value of 3.2 for September and 2.6 for May confirmed the high variability and heterogeneity of the high-pressure centers during the activity of Sistan 120-day winds (Table 1). The maximum and minimum occurrence of the high-pressure centers was at the beginning and end of the activity of Sistan 120-day winds, being 1020.1 and 1014.1 hPa, respectively. Table 2 shows the statistical analogues of the low-pressure centers during the activity of the 120-day winds of Sistan. The minimum and maximum occurrence of the low-pressure centers during the activity of 120-day winds of Sistan occurred in September and May, being 1001.9 hPa and 1007.3 hPa, respectively. The average value of the low-pressure centers was 1004.7 hPa in May. The low-pressure centers with 2% had a lower spatial coefficient of variation compared to the high-pressure ones during the activity of 120-day winds of Sistan that occurred at the beginning and end of the activity of the Sistan 120-day winds (Table 2).

An investigation of low-pressure and high-pressure frequency maps during the activity of 120-day winds of Sistan showed that high- and low-pressure centers are located at above 35° latitudes N and below 30° latitude N. Figure 3 depicts the spatial distribution of the occurrence frequency of low- and high-pressure centers during the activity of 120-day winds of Sistan (May to September). It was found that the maximum frequency of occurrence of low- and high-pressure centers is in July and August, respectively. The lowest frequency of pressure

centers belonged to May and September. Therefore, July can be considered as the month in which 120-day winds of Sistan are at their maximum activity. In late-May, the maximum frequency of occurrence of high-pressure centers was seen in northern Turkmenistan and parts of Uzbekistan. A large part of the high-pressure region experienced a frequency of 0-60. In the same month, the maximum frequency of the occurrence of low-pressure centers was seen over Pakistan between the cities of Hyderabad and Karachi. Certain parts of the central Pakistan had the maximum frequency. A large part of the low-pressure regions had a frequency of 0-50. In Iran, around Zahedan, there is a frequency of 50-100.

Table 1. Statistical characteristics of high-pressure centers in the activity period of 120-day of Sistan wind

H	Oct.	Sep.	Aug.	Jul.	Jun.	All
Average	1016.0	1017.1	1016.9	1016.8	1017.7	1016.9
Median	1016.1	1017.1	1016.9	1016.8	1017.5	1017.0
Mode	1014.1	1015.6	1015.7	1016.8	1015.4	1017.3
STD	1.1	0.7	0.7	0.8	1.0	1.8
CV	1.2	0.5	0.4	0.6	1.1	3.3
Max	1019.2	1018.6	1018.2	1018.2	1020.1	1025.9
Min	1014.1	1015.6	1015.7	1014.8	1015.4	1010.0
Skewness	0.5	-0.1	0.1	-0.4	0.1	0.1
Kurtosis	3.2	2.4	2.0	2.7	2.6	3.5
Range	5.1	3.0	2.5	3.4	4.7	15.9

Table 2. Statistical characteristics of low-pressure centers during the activity of 120-day wind of Sistan

L	Oct.	Sep.	Aug.	Jul.	Jun.	All
Average	1001.9	1002.7	1004.7	1005.7	1007.3	1004.5
Median	1001.9	1002.9	1004.8	1005.9	1007.3	1004.4
Mode	998.5	1000.0	1000.0	1001.2	1007.1	1004.5
STD	1.4	1.0	1.1	1.3	1.4	2.7
CV	2.0	1.0	1.3	1.7	2.0	7.3
Max	1004.9	1004.4	1006.6	1008.4	1009.9	1012.3
Min	998.5	1000.0	1000.0	1001.2	1001.9	994.8
Skewness	-0.2	-0.8	-1.5	-1.1	-0.8	0.0
Kurtosis	3.0	3.3	7.3	5.7	5.1	2.8
Range	6.4	4.4	6.6	7.2	7.9	17.5

In June, as in the previous month, the maximum frequency of the occurrence of high-pressure centers was observed in northern Turkmenistan and parts of Kazakhstan. However, the frequency of the occurrence of high-pressure was doubled compared to that in the previous month. Like May, a large part of the high-pressure activity areas had a minimum frequency of 0-120. In June, the occurrence frequency of the low-pressure centers was roughly tripled and its maximum was seen in central Pakistan. It could be inferred that the maximum occurrence of the low-pressure centers moved from southeast to central parts of Pakistan. A large part of the low-pressure activity area had a minimum frequency of 0-140 (Figure 3). In May, as in the previous two months, the occurrence frequency of the maximum of high-pressure centers was in northern Turkmenistan and parts of Kazakhstan. July had the maximum frequency of occurrence of high-pressure centers during the activity of 120-day winds, with more than 600 occurrences. The frequency of occurrence of low-pressure centers was more than 600. A large part of the region had a frequency of 0-180 (Figure 3). In September, the occurrence frequency of the high-pressure centers decreased compared to that in May. The location of the maximum frequency of occurrence of the high-pressure centers was the same as that in the previous months. In this month, the occurrence frequency of the low-pressure centers also decreased compared to that in the previous month and the maximum occurrence frequency of the low-

pressure centers was still located at the central parts of Pakistan. It seemed as though 120-day winds of Sistan start to weaken in September. The condition of occurrence frequency of the low- and high-pressure centers in September was almost similar to that of May (Figure 3). In fact, the minimum frequency of the low- and high-pressure centers was observed in both months. Nonetheless, the location of the maximum frequency of the low-pressure centers was different with that of May, which was located in the center of Pakistan, like the previous months. The highest average value of pressure difference belonged to September while the lowest was in May. Table 3 demonstrates the continuity of dusts of the studied stations during the activity of 120-day winds of Sistan. At all the stations, the maximum frequency was observed in 2-day dust continuity. The maximum frequency of dusty days was reported in Zabol station. This station even experienced 15 days of dust continuity. Zabol station is located in east of Helmand basin. The longest continuity of the dusty days in Zahedan and Zahak stations was 12 and 11 days, respectively. The lowest continuity of the dusty days was recorded in Deh-e Salam station in the western part and out of the basin and Sarbisheh station in north of the basin (with a 2-day continuity). It should be noted that these stations had a short statistical period and the lack of dusty days could be attributed to this fact.

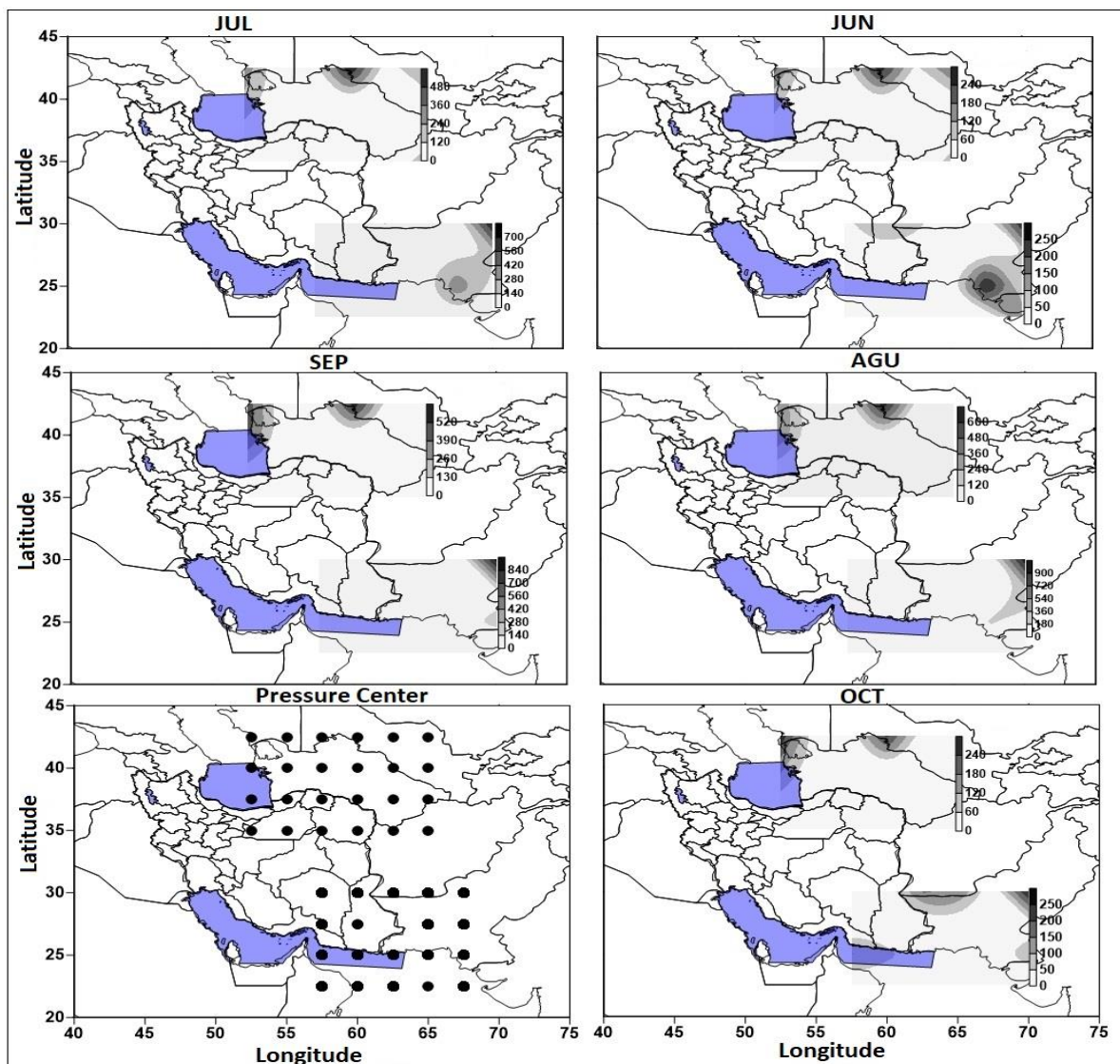


Figure 3. Spatial distribution of high frequency and high pressure occurrence during the activity of 120-day winds of Sistan

Table 3. Persistence of dust in the studied stations during the activity of 120-day winds of Sistan

Persistence of dust (day)	Birjand	Sarbisheh	Nehbandan	Deh-e Salam	Zabol	Zahak	Nosrat Abad	Mirjaveh	Zahedan
2	87	1	32	1	1556	368	112	45	607
3	38	0	12	0	1116	223	65	12	310
4	16	0	6	0	842	128	35	3	165
5	6	0	2	0	671	75	17	0	94
6	2	0	1	0	553	47	7	0	53
7	0	0	0	0	473	27	2	0	29
8	0	0	0	0	407	14	0	0	17
9	0	0	0	0	360	9	0	0	11
10	0	0	0	0	322	4	0	0	6
11	0	0	0	0	290	1	0	0	2
12	0	0	0	0	265	0	0	0	1
13	0	0	0	0	200	0	0	0	0
14	0	0	0	0	130	0	0	0	0
15	0	0	0	0	97	0	0	0	0

Table 4. Frequency and mean occurrence of different types of winds during Sistan's 120-day wind activity

Frequency	Birjand	Sarbisheh	Nehbandan	Deh-e Salam	Zabol	Zahak	Nosrat Abad	Mirjaveh	Zahedan
Light air	805	19	703	49	596	320	26	575	19
Average(m/s)	1.10	1.1	1	1.0	0.9	0.9	1.1	1.1	1.1
Light breeze	3103.00	227	1564	232	1137	640	205	3115	536
Average(m/s)	2.48	2.6	2.3	2.59	2.43	2.40	2.5	2.4	2.6
Moderate breeze	2223	392	834	216	1136	639	357	2184	737
Average(m/s)	4.21	4.3	4.2	4.3	4.3	4.3	4.2	4.2	4.1
Light wind	562	153	453	102	1212	546	125	715	163
Average(m/s)	6.3	6	6.6	6.5	6.6	6.6	6.3	6.4	6.3
Moderate wind	116	51	207	3	1339	478	16	231	18
Average(m/s)	8.9	9	8.9	8.6	9.2	9.1	8.6	8.9	8.7
Strong wind	32	13	43	1	663	305	8	56	-
Average(m/s)	12.2	11.8	11.8	11	12.0	12.0	11.9	11.9	-
Severe wind	3	3	5	-	183	107	-	10	-
Average(m/s)	14.2	15.	14.7	-	15.1	14.9	-	15.3	-
Stormy wind	-	-	-	-	58	20	-	3	-
Average(m/s)	-	-	-	-	18.4	18.2	-	18.6	-
Storm	-	-	-	-	14	8	-	2	0
Average(m/s)	-	-	-	-	-	22.5	21.68	-	23.0
Strong storm	-	-	-	-	4	10	-	1	-
Average(m/s)	-	-	-	-	27.2	26.6	-	24.6	-
Severe storm	-	-	-	-	-	6	-	-	-
Average(m/s)	-	-	-	-	-	30.1	-	-	-
Hurricane	-	-	-	-	1	-	-	-	-
Average(m/s)	-	-	-	-	38.8	-	-	-	-

Table 4 exhibits the average and frequency of the occurrence of different types of winds during 120-day winds of Sistan. Wind speeds at each station were classified according to the same station's data; for example, the average speed of airflow at Zabol and Zahedan stations was 0.95 and 1.19 m/s, respectively. Accordingly, the conditions of each station were indirectly considered in this classification.

It can be inferred from Table 4 that the maximum occurrence frequency of the winds was in different types of low-speed winds. As the wind speed increased, its frequency decreased, such that in some stations, stormy and stronger winds were not recorded.

The maximum frequency of occurrence in Mirjaveh station was 3115 cases, with light breeze, followed by Zabol and Zahak stations that experienced hurricane winds. These two stations are located at the easternmost part of the region. According to the location of the above-mentioned stations, it can be said that the winds are stronger in the eastern parts of the region. Deh-e Salam station did not experience any type of strong winds. This station is located on the west and outside the basin. In addition, the stations located in the west of the basin had less strong winds.

Therefore, wind speed increases from west to east. Table 5 shows the trends of different winds during the activity of 120-day winds of Sistan. As shown, in most of the stations, winds have an increasing trend, which could be attributed to the increase in dusty days in the basin. The results of Table 6 also support this claim. The maximum significant increasing trend belonged to the strong wind at Birjand station and the storm at Mirjaveh station. The minimum significant decreasing trend was observed in the slow airflow at Nosrat Abad and Zahedan stations.

According to Table 5, 19 cases of decreasing trend occurred in low-speed winds and all high-speed winds experienced an increasing trend. The rise in strong winds and storms would increase dusty days. This is because wind is one of the causes of atmosphere moisture movement and can enhance environment dryness, which is one of the factors leading to the formation of dust storm in different regions. As mentioned earlier, the trend of Helmand basin dusts (Table 6) confirms the aforementioned explanations.

Table 5. Trends of types of wind during the activity of 120 cysts

Types of wind	Birjand	Sarbisheh	Nehbandan	Deh-e Salam	Zabol	Zahak	Nosrat Abad	Mirjaveh	Zahedan
Light air	-0.012*	-0.022*	0.028*	0.374*	0.038*	0.056*	-1.156*	0.009*	-0.702*
Light breeze	0.0007	-0.0157*	-0.0061*	0.0560*	0.0199*	-0.0128*	0.0759*	0.0053*	-0.0453*
Moderate breeze	0.0064*	-0.0177*	0.0146*	-0.0030	-0.0176*	-0.0012	-0.0114*	-0.0064*	-0.0072*
Light wind	0.0043	0.1023*	0.0321*	-0.0102	-0.0051*	-0.028*	0.0944*	-0.0109*	0.0563*
Moderate wind	0.6950*	1.1258*	0.1779*	0.26*	0.0793	0.0182*	1.7059*	0.0271*	0.7895*
Strong wind	0.1924*	0.7802*	0.1966*	-	0.4745*	0.0033*	1.5238*	0.0315*	-
Severe wind	1.75*	2*	1.05*	0.83*	0.036*	0.017*	-	1.02*	-
Stormy wind	-	-	-	-	0.032*	0.695*	-	1.5*	-
Storm	-	-	-	-	0.127*	1.595*	-	1.75*	-
Strong storm	-	-	-	-	1.2*	0.8*	-	-	-
Severe storm	-	-	-	-	-	0.023*	-	-	-
Hurricane	-	-	-	-	-	-	-	-	-

* Significant (0.05)

Table 6. Trends of Helmand basin dusts

Station	Trend	Station	Trend
Birjand	0.85	Zahak	3.29*
Sarbisheh	1.54*	Nosrat Abad	2.21*
Nehbandan	1.74*	Mirjaveh	0.624
Deh-e Salam	1.52*	Zahedan	1.55
Zabol	2.48*		

* Significant (0.05)

Table 6 indicates that Zahak and Zabol stations (at the east of the basin) have the maximum significant increasing trend of dusty days. Therefore, the increasing trend of dusty days in the east of the basin is more severe. Generally, the increasing trend of strong winds in Helmand basin has made this region more susceptible to dust storms. Lack of vegetation due to prolonged droughts and low soil moisture has made soil stabilization difficult.

Figure 3 represents the simultaneous correlation and 1- to 3-day delays of pressure gradient and wind speed during the activity of 120-day winds, indicating a direct relationship between the pressure gradient and wind speed in the region. This is because as the pressure gradient of the two regions increases, the speed of air flow between these two regions also rises (Ghaemi, 2007). The study of Tavousi et al. (2012) showed that the increase in wind speed occurred once there was a great pressure difference between Sistan and the northeastern regions. This relationship was stronger as simultaneous, but with the increase in the delay, it decreases. Simultaneous correlation coefficient in the east of the basin showed a strong relationship. This relationship had the lowest value in the south of the basin. Regarding the correlation coefficient with 2 days of delay, the center of the maximum moved to the western part of the northern half of the basin. For the correlation coefficient with 3 days of delay, the maximum relationship was seen in the east of the basin. However, the northern and southern areas of the basin showed weaker relationships (Figure 4).

Figure 5 illustrates the simultaneous correlation and 1- to 3-day delays of pressure gradient and dusts during the activity of 120-day winds. This figure indicates the direct relationship between pressure gradient and dust in the region. The study of Alijani and Raispour (2011) revealed that dust storm was intensified in Sistan region during the creation of high-pressure gradient between the northern high-pressure centers and Indian-Pakistani seasonal low-pressure ones. Moreover, Mofidi and Kamali (2012) attributed the increase in high-pressure gradient between Turkmenistan high-pressure and Pakistan low-pressure as the cause of Sistan dust storms. This relationship was stronger simultaneously, and as the delay increased, it weakened; it reached its lowest level in 3 days of delay. For simultaneous correlation coefficient and with 1- to 3-day delays, the east of the basin had the highest correlation value. This relationship in the south of the basin, with simultaneous correlation coefficient and 1- to 2-day delays, was weaker than that in the other parts of the basin. For the correlation coefficient with a 3-day delay, the northern belt of the basin had the weakest relationship compared to the other parts of the basin. The increase in pressure gradient resulted in a rise in wind speed. In addition, since Sistan region has been suffering from drought for many years, its soil was poor in moisture and cannot withstand erosion by strong winds. Thus, the formation of strong winds in this region would lead to the transportation of dust to the atmosphere and formation of dust storms.

Conclusion

120-day wind of Sistan has several positive and negative ecological effects. In fact, this wind is a middle-atmospheric phenomenon. By blowing continuously, it contributes alternatively to dust dense, reduction in visibility of view, and increase in mineral pollutants in Sistan Plain and a large region of western Afghanistan and northwest Pakistan. Therefore, this study aimed to investigate the relationship between the pressure gradient of these two sources and their effects on wind speed and dust. Based on the frequency map of the low- and high-pressure centers affecting 120-day winds of Sistan, the maximum frequency of occurrence of these centers was observed in July and August, respectively. May and September had the minimum frequency of pressure centers. Accordingly, July could be considered as the month when 120-day winds of Sistan were at their maximum activity.

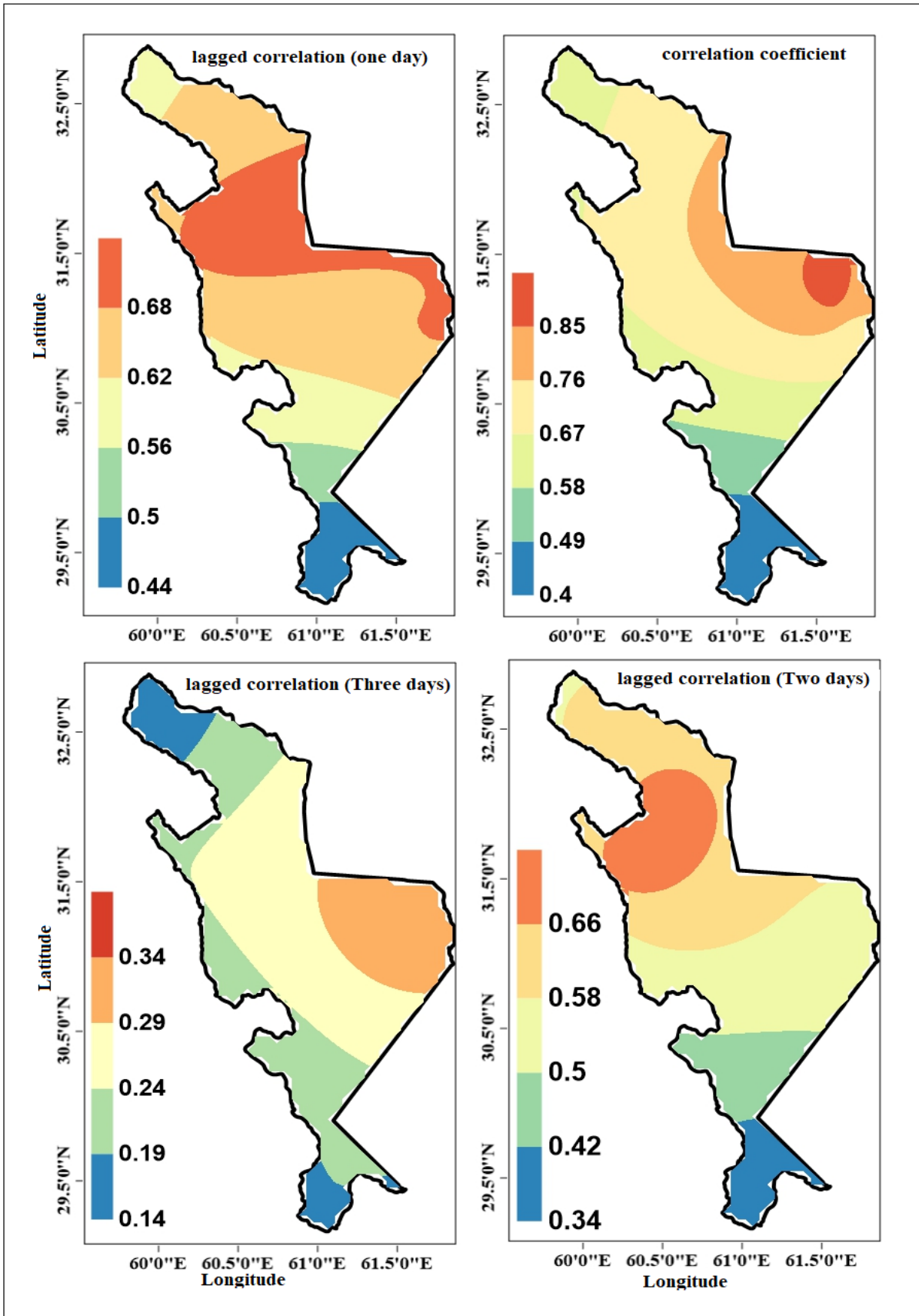


Figure 4. Correlation coefficient between pressure gradient and wind speed

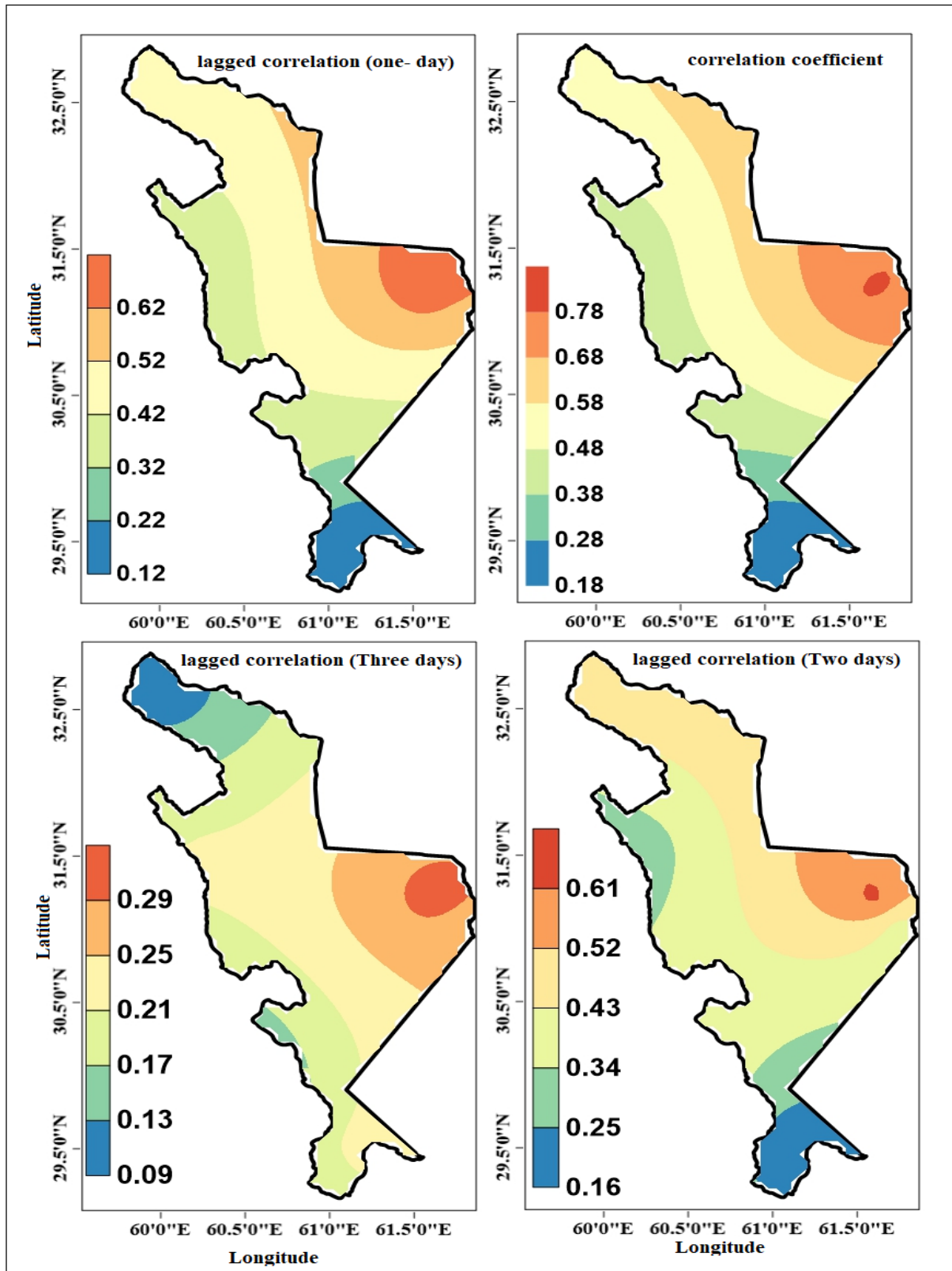


Figure 5. Correlation coefficient between pressure gradient and dust

The maximum frequency of high-pressure centers was located in northern Turkmenistan and parts of Uzbekistan. Meanwhile, the maximum frequency of low-pressure centers, except in July, was located in the central regions of Pakistan. This center with the maximum frequency was seen in southern Pakistan between Hyderabad and Karachi in July.

Studies have shown that slow winds had the maximum frequency. Furthermore, strong winds had further frequency in the east of the basin, in Zabol and Zahak stations. Only Zabol station experienced a 15-day continuity. The maximum frequency of continuity was also recorded at Zabol station. Slow winds had a decreasing trend whereas strong winds had an increasing one. This could be one of the factors increasing dusty days. The rising trend of dust at basin stations confirmed this claim.

Investigation of simultaneous and 1- to 3-day delays relationship of pressure gradient during the activity of 120-day wind with wind speed and dust showed the direct relationship of pressure gradient with dust and wind speed. The relationship was strong simultaneously and weak with delays. Moreover, this relationship was strong in the east of the basin and weak in the west. Generally, pressure gradient during the activity of 120-day winds could up to an extent influence the formation of wind and dust in the basin. The findings of many researchers confirmed the results of this study. They believe that the blowing of northern to northwestern winds is due to the pressure difference between the seasonal low-pressure source located in southern Iran and Pakistan and high-pressure centers of Caspian Sea to Central Asia and North Afghanistan (Saliqeh, 2010; Khosravi, 2010).

Reference

- Alijani B, Raispour K. 2011. Statistical and Synoptic Analysis of Dust Storms in Southeastern of Iran (Case Study: Sistan Region). *Geographical Studies of Dry Areas*, 5; 107-132.
- Alizadeh A. 2009. *Principles of Applied Hydrology*, Astan Quds Razavi Publications, Mashhad, Iran.
- Anaxos, Inc. 2008. *UXL encyclopedia of weather and natural disasters*.
- Arnes CD. 2012. *New Meteorology Introduction to Air, Climate and Environment*. Translated by Mohammad Reza Babaei. Aizeh Publications, Tehran, Iran.
- Brazel AJ, Nickling WG. 1986. The relationship of weather types to dust storm generation in arizona (1965-1980). *Journal of Climatology*, 6; 255-275.
- Diaz-Hernandez JL, Sanchez-Navas A. 2016. Saharan dust outbreaks and iberulite episodes, *J. Geophys. Res. Atmos*, 121; 7064–7078.
- Gandmakar A. 2009a. Synoptic study of wind energy in Sistan region (Zabol station). *Geographical space*, 27; 161-180.
- Gandmakar A. 2009b. Wind potential energy assessment in Iran. *Geography and Environmental Planning*, 36; 85-100.
- Gandmakar A. 2010. Investigation of air patterns governing Sistan wind using cluster analysis. *Geographical Landscape*, 12; 101-116.
- Ghaemi H. 2007. *General Meteorology*, Samat publications, Tehran, Iran.
- Hosseinzadeh, S, 1997. 120-Day Winds of Sistan, *Geographical Research*, 47; 103-127
- Jalali N, Iranmanesh F, Davoodi MH. 2017. Identifying the Origin and Areas Affected by Dust Storms in Southwestern of Iran Using MODIS Images. *Journal of Watershed Engineering and Management*, 9(3); 318-331.
- Kaykhosravi Gh, Haseli M. 2017. Trajectory simulation of some examples of severe dust storms in Kermanshah province from the perspective of HYSPLIT model. *Natural Geography Quarterly*, 10 (37); 59-82.
- Kellogg PJ, Goetz K, Monson SJ. 2016. Dust impact signals on the wind spacecraft. *J. Geophys. Res. Space Physics*, 121; 966–991.
- Khosravi M. 2010. Study of vertical distribution of dust caused by storms in the Middle East using NAAPS model Case: Sistan Iran, 4th International Congress of Geographers of the Islamic World, Sistan and Baluchestan University, Zahedan, Iran.
- Littmann T. 1991. Dust Storm Frequency in Asia: Climatic Control and Variability. *International Journal of Climatology*, 11; 393-412.
- Meloni D, Junkermann W, di Sarra A, Cacciani M, De Silvestri L, Di Iorio T, Estellés V, Gómez-Amo JL, Pace G, Sferlazzo DM. 2015. Altitude-resolved shortwave and longwave radiative effects of

- desert dust in the Mediterranean during the GAMARF campaign: Indications of a net daily cooling in the dust layer, *J. Geophys. Res. Atmos.*, 120; 3386–3407.
- Miri A, Moghaddamnia A, Pahlavanravi A, Panjehkeh N. 2010. Dust storm frequency after the 1999 drought in the Sistan region, Iran. *Clim Res* 41; 83–90.
- Mofidi A, Kamali S. 2012. Investigation and analysis of the structure of dust storms in Sistan plain using the regional climate model RegCM4; Case Study: July 30, 2001, The First National Desert Conference, Karaj, Iran.
- Pokharel AK, Kaplan ML, Fiedler. 2017. Subtropical dust storms and downslope wind events. *Journal of Geophysical Research: Atmospheres*, 122(10); 191- 205.
- Prakash, Jish P, Stenchikov G, Kalenderski S, Osipov S, Bangalath H. 2015. The impact of dust storms on the Arabian Peninsula and the Red Sea. *Atmos. Chem. Phys.*, 15; 199–222.
- Raigani B, Kheirandish Z, Kermani F, Mohammadimiab M, Torabinia A. 2016. Identification of actual foci of dust production using remote sensing data and airflow simulation Case: Alborz Province. *Journal of Desert Management*, 8; 15-26.
- Refahi H. 2009. *Wind Erosion and its Control*, University of Tehran Press, Tehran, Iran.
- Saliqeh M. 2010. Joint Effects of Thermal Interaction of Atmospheric Systems in Islamic Countries: A Case Study: 120 Days of Sistan Winds, 4th International Congress of Geographers of the Islamic World, Zahedan. Iran.
- Shahriari A, Mohammadi M. 2015. A Study of the Time Series of Dust Phenomena in Sistan and Baluchestan Province Using Nonparametric Statistical Methods. *Journal of Soil and Water Conservation Research*, 22(4); 253-260.
- Tavousi T, Safarzaei N, Raispour K. 2010. Statistical Analysis of Dusty Days in Sistan during the period (1976-2005), 4th International Congress of Geographers of the Islamic World, Zahedan. Iran.
- Tavousi T, Saliqeh M, Safarzaei N. 2012. Investigation of wind vector parameters and its role in dust storms in Sistan, Iran. *Geography and environmental stability*, 2; 19-30.
- Wang X, Schwan J, Hsu HW, Grün E, Horányi M. 2016. Dust charging and transport on airless planetary bodies. *Geophys. Res. Lett.*, 43' 6103–6110.
- Zeinali B. 2016. A study of the trend of changes in the frequency of days associated with dust storms in the western half of Iran. *Journal of Natural Environment Hazards*, 5(7); 87- 99.
- Zomordian MJ. 2002. *Geomorphology of Iran*. 4th ed., Ferdowsi University Press, Mashhad, Iran.